BS 2021 1-3 SEPT BRUGES

INTERNATIONAL BUILDING PERFORMANCE SIMULATION ASSOCIATION

Solar Radiation Nowcasting through Advanced CNN Model Integrated with ResNet Structure

Lei Chen[1], Yangluxi Li[1], Hu Du[1], Yu-Kun Lai[2]
[1]Welsh School of Architecture, Cardiff University, Cardiff, United Kingdom
[2]School of Computer Science and Informatics, Cardiff University, Cardiff, United Kingdom

Abstract

Although a range of solar radiation forecasting methods have been developed for predicting photovoltaic generation, only a few of them focus on solar radiation forecasting for building energy demand. From the perspective of building performance modelling, solar radiation forecasting needs to meet several critical requirements including high spatial resolution (1m-2km) and high temporal resolution (5-60mins), the accurate value of Direct Normal Irradiance (DNI) and Diffuse Horizontal Irradiance (DHI), which differs the requirement for predicting photovoltaic generation. As the geometric sum of DNI and DHI, accurate prediction of Global Horizontal Irradiance (GHI) with high spatial-temporal resolution tends to be the prerequisite for precise prediction of DNI and DHI.

This research aims to construct a hybrid nowcasting model to predict GHI in high spatial-temporal resolution. In this article, the authors adopt an advanced Convolutional Neural Network (CNN) model with Residual Neural Network (ResNet) structure to identify the cloud image information and predict the GHI at 10 minutes intervals merely using cloud images captured by a ground-based sky camera. On this basis, several ResNet structures are compared to achieve the optimal nowcasting model for GHI.

The results present that the ResNet structure can efficiently capture the cloud information and the ResNet-152 achieves better performance than other alternative structures on the nowcasting of GHI.

Finally, the authors discussed the calculation of synchronous DNI and DHI using the predictive GHI and Dirint model, and the application of DNI and DHI as the input for the simulation of building energy management.

Key Contributions

- Classifying solar radiation forecasting methods and reviewing recent representative articles.
- Proposing a hybrid method using CNN-ResNet models to nowcast solar irradiance.
- Only using ground-based cloud images as input to predict solar irradiation.
- Comparing several ResNet structures to achieve the optimal nowcasting model for GHI.

Practical Implications

This study makes it possible for relevant researchers to utilise predictive solar radiation data in a convenient manner, taking only cloud images as input instead of other difficult-to-obtain weather data.

Introduction

Due to the increasing cost and carbon emission of conventional fossil energy, renewable energy has gradually gained increasing interest in the research community (Leirpoll, et al., 2021), including architecture (Song & Song, 2020). As the representation of renewable energy sources, solar energy has great potential capacity to building energy management (Guermoui, Melgani, & Danilo, 2018). In building energy management, high spatial-temporal resolution GHI, DNI and DHI are the critical input parameters for achieving high-performance buildings through model predictive control (Du, Bandera, & Chen, 2019). However, accurate prediction of solar radiations at ground level has always been a challenging task considering the dynamic nature of cloud movement, water vapour and pollution of the air. In this case, many solar radiation forecasting methods have been developed in the past decades which achieved decent performance in their designated spatial and temporal horizons.

Forecasting Methods for Solar Radiations

A series of research have provided comprehensive reviews on solar radiation forecasting methods and proposed their classification of solar radiation forecasting methods (Diagne, David, Lauret, Boland, & Schmutz, 2013) (Antonanzas, et al., 2016) (Yang, Kleissl, Gueymard, Pedro, & Coimbra, 2018). Refer to the viewpoints of the above research, solar radiation forecasting methods are classified into the following categories in this article:

- Numerical Weather Prediction methods (NWPs)
- Statistical and Learning methods
- Top-down methods
- Bottom-up methods
- Hybrid methods

Numerical Weather Predictions methods (NWPs) are mainly based on the mathematic models of the atmosphere and oceans to predict the weather in the future. The application of NWPs on solar radiation forecasting has the most extended history. It is often only used in large national institutions due to the requirement of

https://doi.org/10.26868/25222708.2021.30732

supercomputers for complex calculation. Therefore, NWP methods are suitable for macroscopical and long-term forecast. Global Forecast System (GFS) and Weather Research and Forecasting (WRF) are representative models of NWPs.

Due to the rapid development of computer techniques, Statistical and Learning methods have emerged in the last several decades. Statistical and Learning methods essentially analyse the pattern of historical data to predict future data. The most representative statistical methods involve Autoregressive Moving Average (ARMA) and Autoregressive Integrated Moving Average (ARIMA). Typical Learning methods include Support Vector Machines (SVM), Decision Trees, Artificial Neural Networks (ANNs) and Convolutional Neural Networks (CNNs). In general, for discrete models, Statistical and Learning methods can perform well in various spatial-temporal resolution as long as the data samples have the appropriate spatial-temporal resolution.

Top-down methods refer to the analysis of satellite cloud images obtained from the atmosphere above. Through examining two consecutive cloud images captured by the meteorological satellite, cloud motion can be tracked. Then, cloud motion is used to achieve predictive cloud cover information which is finally translated into the solar radiation forecast through mathematic models. The use of satellites means these methods have a good performance on regional and middle-term solar radiation forecasting.

Bottom-up forecast methods, which share the similar principles to Top-down methods, have emerged in recent years because of their potentials for providing high spatial-temporal resolution solar radiation forecasting. The significant distinctions between Top-down and Bottom-up methods are camera position and photograph intervals. Typically, for bottom-up methods, a ground-based all-sky camera called "Total Sky Imager" (TSI) is used to photograph cloud images from the ground. Similar to the principle of ordinary cameras, TSI can photograph cloud information at the intervals from one second to several minutes, and the captured images are then used for predicting solar radiation in very short-term temporal horizons from one second to several minutes.

Hybrid methods usually consist of two or more of the above methods for taking advantage of the strengths of each methodology. In recent years, a series of Hybrid methods have demonstrated their superior performance for predicting forecasting high-quality solar radiation.

Table 1 shows a series of representative studies on solar radiation forecasting between 2018 and 2021. More early literature review can refer to a previous study (Chen, Hu, & Li, 2019). Table 2 demonstrates the ability of different forecasting methods in various spatial-temporal horizons.

Solar Irradiance Components

Solar radiation forecasting mainly refers to three crucial solar irradiance components: Global Horizontal Irradiance (GHI), Direct Normal Irradiance (DNI) and Diffuse Horizontal Irradiance (DHI). GHI is the total irradiance from the Sun on a horizontal surface on Earth. DNI is measured at the surface of the Earth at a given location with a surface element perpendicular to the Sun. DHI is the radiation at the Earth's surface from light scattered by atmospheric components, such as molecules and particles. The relationship between GHI, DNI and DHI can be expressed as:

$$GHI = DHI + DNI \times \cos(\theta) \quad (1)$$

where θ is the solar zenith angle.

Research Gaps of Forecasting Methods for Solar Radiations

Based on the review of various forecasting methods for solar radiations, a range of significant research gaps are summarised as follows:

Firstly, only a few studies focus on both spatial and temporal resolution of solar radiation forecasting.

Secondly, the data acquisition for most studies tends to require complex data types and high-cost equipment.

Finally, very few studies discuss the generation of DNI and DHI nowcasting from GHI nowcasting and the application of DNI and DHI nowcasting for the simulation of building energy management.

In fact, filling the above research gaps of solar radiation forecasting is significant to the optimisation of building energy management. (Kim, Katipamula, & Lutes, 2020) indicates that the solar radiation forecast is crucial for intelligent load control to manage building loads. At first, unlike the huge scale infrastructure, such as regional grids, building energy management requires high spatial-temporal resolution of solar energy information. Thus, the nowcasting of solar radiation ranges from 5 to 30 minutes in a specific spatial horizon from 1 meter to 2km. In addition, most simulation software for building requires specific DNI and DHI as input parameters due to the orientation of buildings. In the end, most of the individual buildings are impossible to afford expensive equipment for solar data acquisition. To sum up, it is worth exploring a solar radiation nowcasting method to meet the specific needs of building energy management.

The Potential of Hybrid Nowcasting Method for Solar Radiations

Therefore, this research aims to develop a hybrid nowcasting model to predict GHI in high spatial-temporal resolution. Due to the page limit, this paper focuses on the construction of the hybrid nowcasting model.

The hybrid nowcasting model investigated in this paper mainly combines two major solar forecasting methods: Statistical methods and Bottom-up methods. Firstly, Bottom-up method use a ground-based sky camera to capture the cloud images in 10 minutes interval with 2km image range. Secondly, convolution neural network (CNN), which is a representative Learning method, is applied to learn the relation between cloud image and next time-step measured GHI. In the end, several ResNet structures of CNNs are compared to achieve the optimal nowcasting model for GHI. In this way, the high spatial-temporal resolution nowcasting of GHI are achieved.

https://doi.org/10.26868/25222708.2021.30732

Table 1 Solar radiation forecasting methods developed recently (2018-2021)

Paper	Parameter	Frequency	Data Resource	Crucial Approach
Numerical Weather Prediction (NWP) Methods				
(Miller, Rogers, Haynesa, Sengupta, & Heidinger, 2018)	DNI, DHI	Hourly, 3-hour	Public Meteorological Observations	CIRACast
(Pereira, Santos, & Rocha, 2019)	GHI	Hourly	Public Meteorological Observations	WRF OCP
Statistical and Learning Methods				
(Yu, et al., 2018)	GHI	Hourly	Weather Application Programming Interface (API)	BPN RBFNN ENN
(Zalata , Robandi, & Riawan, 2018)	GHI	Hourly	Weather Application Programming Interface (API)	ANN
(SORKUN, İNCEL, & PAOLI, 2020)	GHI	Hourly	Public Meteorological Observations	Deep Learning LSTM
(Miriyala, Nagalla, & Mitra, 2019)	GHI	Hourly	Weather Application Programming Interface (API)	Optimal Long Short Term Memory Networks
Top-Down Methods				
(Kallio-Myers, Riihelä, Lahtinen, & Lindfors, 2020)	GHI	15-min	Meteorological Satellite	Satellite Cloud Image
(Alonso-Montesinos , Polo, Ballestrín, Batlles , & Portillo, 2019)	DNI	15-min	Meteorological Satellite Privately-owned Measurement	Satellite Cloud Image
Bottom-Up Methods				
(Bone, Pidgeon, Kearney, & Veeraragavan, 2018)	DNI	Hourly	Ground-based Total Sky Imagers	Ground Cloud Image
(Caldas & Suarez , 2019)	GHI	1-min	Ground-based Total Sky Imagers	Ground Cloud Image
(Wang, et al., 2020)	GHI	1-min	Ground-based Total Sky Imagers	Ground Cloud Image
Hybird Methods				
(Kwon, Kwasinski, & Kwasinski, 2019)	GHI	1-hour	Weather Application Programming Interface (API)	Nave Bayes Classifier
(Wu, Li, & Xia, 2021)	GHI	1-hour	Weather Application Programming Interface (API)	MTS-ESN
(Gentile, et al., 2020)	GHI	Hourly	Meteorological Satellite	WRF-ARW
(Wang, et al., 2019)	GHI	10-min	Ground-based Total Sky Imagers	CNN LSTM
(Leelaruji & Teerakawanich, 2020)	GHI	1-2-min	Ground-based Total Sky Imagers	CNN

Table 2 Ability of Different Methods in Various Spatial-Temporal Horizon

Methods	NWP	Statistical & Learning	Top-Down	Bottom-Up	Hybrid
Spatial Horizon	5-20 km	1 m-2 km	1-10 km	1 m-2 km	1 m-20 km
Temporal Horizon	4-36 hours	1 second-1 month	30 mins-6 hours	5-30 mins	1 second-1 month

Methodology

Figure 1 presents the working flow of the proposed hybrid nowcasting model.

Data Acquisition

In this study, National Renewable Energy Laboratory (NREL)'s Solar Radiation Research Laboratory (SRRL) dataset is used as the database. This database was established in 1981 by NREL at the South Table Mountain Campus (longitude: 105.18° W, latitude: 39.74° N, elevation: 1,828.2m) (Stoffel & Andreas, 1981) (Anderberg & Sengupta, 2014). It provides two types of cloud images which were shot by the Yankee Total Sky Imager (TSI-800) with 1-min resolution and the EKO all Sky Imager with a 10-min resolution. Taking consideration of the requirement of this study, it is reasonable to select the cloud images photographed by the EKO Sky Imager as the training images since EKO Sky Imager can shoot an entire sky without shadow-band in a 10-min resolution. The cloud images were captured with a high resolution of 1536*1536. All cloud images are colour images with RGB channels. The NREL database only records the daytime cloud images according to specific weather data. In other words, in different seasons, the recording period of cloud images is variable in line with the daytime length. In this study, cloud images recorded from 6:40 am to 4.30 pm are used. In addition, the cases with negative and zero GHI values in the early morning and late-night are eliminated from the database.

Apart from cloud images, numerical meteorological parameters including GHI, DNI, DHI, temperature, relative humidity, wind speed, etc., are available according to various time scales, such as year, hour, minute. In addition, the Ineichen and Perez clear sky GHI

(Stein, Holmgren, Forbess, & Hansen, 2016) are also provided.

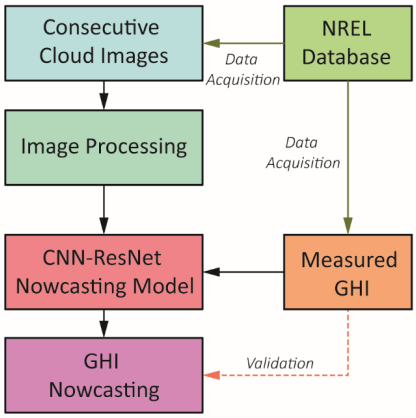

Figure 1 Working flow of hybrid nowcasting model

To successfully train the CNN model, it is essential to avoid the over-fitting problem. The dataset chosen is crucial for model training and testing. From 01/10/2017 to 01/10/2019, monitored numerical values and cloud images in two years are used as the dataset for the model training. Then, images and data in the period of 01/10/2019 to 01/05/2020 are selected as the validation set. Moreover, the remaining data in 2020 plays the role of the testing set. Finally, the sample numbers in the training, validation and testing sets are 35040, 10080 and 11520, respectively. All these data are generated every 10 minutes means the CNN model established in this study predicts GHI 10 minutes ahead with respect to the time resolution.

Convolutional Neural Networks (CNNs)

- Basic working principle

The crucial stage of this article is to predict solar irradiance based on cloud images. As an advanced image recognition approach, CNN (Convolutional Neural Networks) is applied to construct the nowcasting model. It has been proved that CNN has enabled great success in many research fields, such as speech recognition, image recognition (Krizhevsky, Sutskever, & Hinton, 2012), natural language processing (Ronan & Jason, 2008), etc.

CNN can automatically learn features from big data sets and generalise the results to the same type of unknown data. An entire CNN system typically involves multiple convolution sections. Each convolution section contains three structures, namely convolution, activation and pooling. Multiple convolution sections process feature maps in sequence and finally output feature maps that capture high-level information of the input image. After that, this output result is input into a fully connected layer so as to establish the mapping relation between cloud image and solar irradiance. In this case, solar irradiance can be achieved through the analysis of cloud images. Figure 2 presents a typical convolution section's interior logic workflow of the proposed CNN model (ResNet-152). A convolution section can also be called a stage. In general, three maps volume are involved in a stage, as shown in *Table 3*. Different maps volume correspond to different solution functions as well as the structures mentioned above.

Table 3 Maps volume in stage

Map volume name	Purpose	Solution function
Input map volume	Store input image information	Convolution
Feature map volume	Store image information after kernel filtering	Activation
Pooled map volume	Reduce the space of feature maps	Pooling

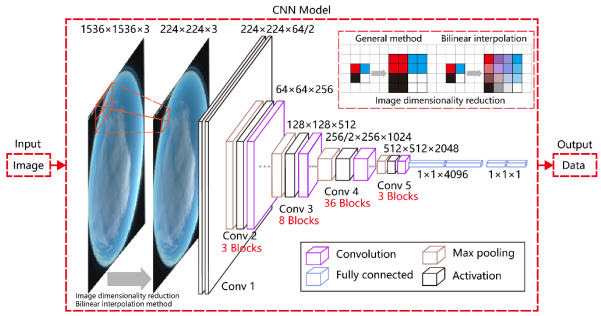

Figure 2 Structure of CNN model (ResNet-152)

- Convolution (Kernel filtering of input images)

The essence of Convolution is Kernel filtering computation process. In this process, the kernel (filter) is the crucial element, which is applied across all the spatial locations and convolutes with input map volume (pixels of images for the first convolution section and feature maps from the previous convolution section otherwise). As convolutions are applied to map volumes, 3-D kernels are used. Take the first convolution section as an example. A 3-D kernel is comprised of multiple 2-D plane kernels. This 2-D component only scans picture pixel data under plane dimensions. That is to say, the 2-D block slides displacements on X and Y instead of axis Z. With respect to image structure, RGB channels form the entire picture colour and the number of pixels controls the size of the image. Combining kernel and image structure, X, Y present the total size of the photo along with horizontal and vertical directions, while RGB channels represent the Z information. Each 2-D image plane requires a 2-D kernel to collect data condition. Therefore, three 2-D kernels performed on three channels with RGB (Red, Green, Blue) and then generate a final feature map after convolution effect for a common photo. In this case, a picture needs a kernel composed of three 2-D kernels to scan. Note that multiple 3-D kernels are typically used to output feature maps with multiple channels.

- Activation (Activation in feature maps volume)

After the convolution step, to introduce non-linearity, an activation function is introduced to calibrate the convolution results for each pixel. In fact, the feature map volume includes feature maps after applying convolution and activation function.

- Pooling

As the feature maps have too complex pixel information after activation, in this phase, pooling operation, in fact as a subsampling manner, intends to decrease the feature

https://doi.org/10.26868/25222708.2021.30732

map resolution. That helps to extract a more informative representation and meanwhile reduces the computational cost. Three commonly used pooling operations are max pooling, average pooling and L2 pooling. Max pooling means choosing the max pixel (or feature) value in a certain range to replace original data. Average pooling refers to selecting the averaged value among certain areas. L2 pooling is to take the mean squared value. It's worth noting that pooling is not indispensable, especially under abundant computing capacity. Currently, some large CNNs only occasionally use pooling.

A basic CNN stage consists of the aforementioned steps. Connecting with each stage constitutes the entire CNN structure. The final output of CNN is feature maps that are input into networks with follow-up classification or regression tasks.

- Fully Connection Layer

Fully Connection Layer appearing in CNN is used to aggregate information for making a global prediction, such as classification or regression. In other words, this network is used for achieving the prediction function, while the convolutional and max pooling layer is responsible for extracting efficient information from cloud images. Combining these two processes, the final solar irradiance forecast result is obtained. Fully Connection Layer establishes the connecting bridge between feature map and GHI values.

The objective function of this study implements the L1 function. Its target minimises the sum of the absolute difference between the target value and the estimated one. Another common objective function is L2 which minimises the sum of squares of the difference between the target and the estimated value. The robustness of L1's loss function is better than L2. The L1 loss function is not easily affected by the observation with significant error. This is because the L1 increases only one error, while the L2 gets the square of the error. When it is large, it needs to adjust the model to a greater extent for accommodating this observation with L2, so the L2 loss function is not as stable as the L1 loss function. In the beginning, the L2 loss function was adopted to train this model and could not reach an ideal result. After changing it to be L1, the model can estimate both the magnitude and trend of irradiation.

ResNet Structure of CNN Model

This study applies the CNN model for solar prediction purpose. Theoretically, more layers in depth are able to enable more learning capabilities for the neural network. However, the degradation problem gradually emerges as the increase of CNN layers significantly affects final forecast accuracy. Degradation problem refers to the problem that as the network depth increases, the final model accuracy gradually changes to be saturated and then degrades rapidly. In brief, the CNN model forecast accuracy level decreases when the number of model layers reaches a threshold value. Meanwhile, once the network has too many layers, the weight values for different neurons tend to be an oversize or undersized condition as an accumulation effect along with layers. In this case, to solve these two issues, a classical CNN model structure of ResNet (Residual Neural Network) was implemented in this research (He, Zhang, Ren, & Sun, 2016). The ResNet structure of the CNN model could overcome this problem and make the number of CNN layer increase without limitation of layers under the premise of remaining forecast precision.

Facing the degradation problem of multiple layers CNN construction, ResNet model integrated residual learning block to figure it out. It can enhance the layer of neutral network model via residual learning, which allows backpropagation to be effectively carried out even when certain neurons are saturated. This design makes it can efficiently learn very deep neural networks and thus outperform traditional CNN models.

Figure 3 Typical structure of ResNet-152 presents a typical structure of the ResNet-152 model. In this research, several ResNet models are evaluated. For example, the ResNet-152 model consists of 152 convolution layers, 2 max pooling layer, 2 averaged pooling layer and 1 fully connection layer. The block indicates the residual block with shortcut mechanism in two layers solving the degradation issue and improving the training efficiency.

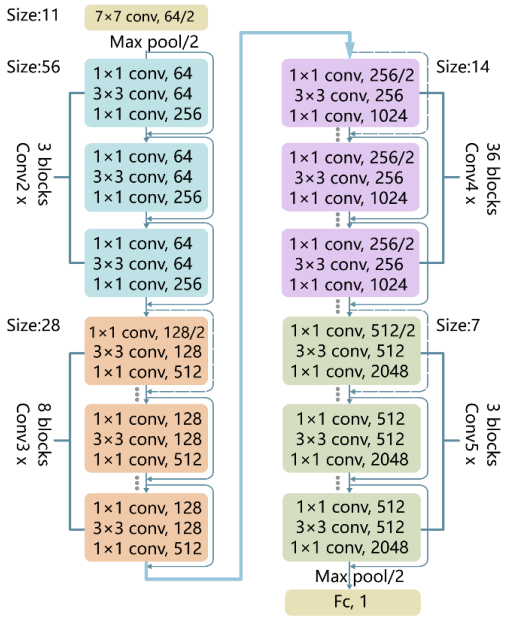

Figure 3 Typical structure of ResNet-152

Using the CNN-ResNet model, this study can predict the Global Horizontal Irradiance (GHI) in 10 minutes ahead only using cloud images.

Result

In this section, the nowcasting results are listed to denote the model performance. In terms of model establishment, Table 4 presents the performance of model training. In this table, the ResNet-number refers to the layer number of corresponding models, as presented in the methodology section. Figure 4 shows the CNN model training result in terms of the loss function. It indicates that the nowcasting model achieves convergence situation at training and validation set after 1000 epochs which only

shows 100 epochs in Figure 4. This phenomenon presents the ResNet-152 model has been optimised in maximum.

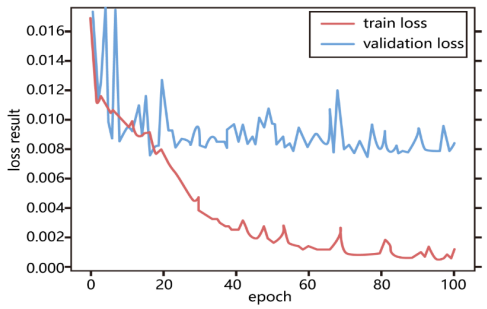

Figure 4 Loss function for ResNet-152 model training

It can be observed from Table 4 the ResNet-152 model has the optimal performance in forecast accuracy regarding performing indicators of Mean Absolute Error (MAE), Root Mean Square Error (RMSE). Although all these ResNet structures have similar R-values that measure the relative ability between variables and predicted value, MAE and RMSE are the primary loss function indicators indicating that ResNet-152 can achieve the optimal forecast condition. For example, the RMSE of ResNet-152 is lower than ResNet-34 by 2.9%.

Table 4 Nowcasting performance of various ResNet

Method	RMSE	MAE	R
ResNet-34	65.88	50.89	0.93
ResNet-50	65.91	50.67	0.93
ResNet-101	64.86	49.26	0.92
ResNet-152	63.98	48.11	0.93

Meanwhile, Figure 5 also presents the comparison between predicted values of the ResNet-152 and measured values in three typical days. All predicted values have a similar trend with measurement data and indicate agreement condition with actual values at a high degree. Coupling with quantity comparison with Table 4, this phenomenon shows that the ability of the ResNet model could achieve superior results via a large number of layers structure. In addition, the final result meets the expectation that the model performance improves with the increase of layer, which presents ResNet-152 has the best forecast ability.

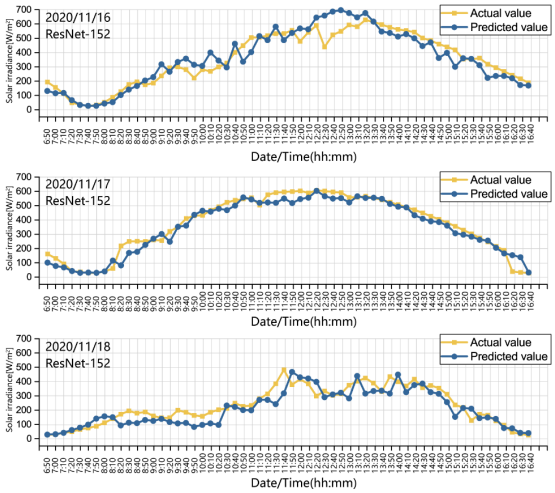

Figure 5 Measured and predicted GHI in typical days

Table 5 presents the sky conditions and nowcasting performance from Nov.16 to Nov.18. On Nov.16, the sky was partly cloudy in the morning and transformed to be clear in the afternoon. On Nov.17, it was sunny all day without thick clouds. On Nov.18, it was overcast throughout the day. It is evident that the nowcasting accuracy on Nov.16 is the worst due to the high variability of sky conditions.

Table 5 Nowcasting performance in three typical days

Date	Sky Conditions	RMSE	MAE	R
Nov.16	Partly Cloudy	67.01	51.31	0.94
Nov.17	Clear	44.56	32.90	0.98
Nov.18	Overcast	55.60	46.60	0.90

Discussion

In this study, the proposed hybrid nowcasting method for GHI mainly includes several advantages compared to other studies.

At first, the classification, comparison and review of various solar radiation forecasting methods in this study provides a comprehensive horizon of this field.

Secondly, the developed nowcasting method using optimised ResNet structure effectively overcomes the limitations of the basic CNN model used in other studies.

In addition, the comparison of several ResNet structures that explore the optimal solution for the nowcasting and provides an in-depth understanding of ResNet models.

Moreover, the proposed nowcasting method only use cloud images as the input parameters that decrease the application difficulty of the nowcasting method in areas without comprehensive meteorological data, such as humidity, wind speed, etc.

Finally, according to the performance evaluation, the proposed nowcasting model can achieve a better RMSE and MAE compared to most similar solar forecasting models.

Utilisation of GHI Nowcasting for Building

In addition to developing the GHI nowcasting method, this study aims to discuss its utilisation for building energy management.

Although most of the current studies usually apply GHI nowcasting for preventing solar energy facilities from ramp events (Kong, Jia, Dong, Meng, & Chai, 2020), the development of computer science and the advanced method of process control, such as Model Predictive Control (MPC), can promote the utilisation of GHI nowcasting for building energy management. (Dong & Lam, 2014) imports the solar radiation value in advance into the building control system to adjust interior equipment parameters. (Kwak, Seo, Jang, & Huh, 2013) adopts the solar forecast to achieve a novel methodology for short-term real-time energy demand prediction using a building simulated program. (Kummert, André, & Nicolas, 2001) utilises predicted solar irradiance condition to control the passive solar commercial building, which adjusts energy efficiency strategy in line with the weather conditions.

Calculation of DNI and DHI from GHI

Due to the location and orientation of buildings, it is worth noting that most simulation software for building energy management, such as Energy Plus, usually require specific values of DNI and DHI rather than GHI or use in-built algorithms to calculate the DNI and DHI from GHI. Hence, it is worth exploring the methods for calculating DNI and DHI from the GHI. (Perez, Ineichen, Maxwell, Seals, & Zelenka, 1992) presented a model named DIRINT successfully split GHI into DNI and DHI at a high precision level. Using the DIRINT model, the authors of this article have calculated DNI and DNI from predicted GHI with reasonable accuracy compared to measurement.

Limitations and Future Work

This study has three main limitations. Firstly, the temporal horizon of the GHI nowcasting was limited to 10 minutes interval. Different temporal horizon ranging from 1 minute to 60 minutes should be tested to verify the performance of this nowcasting model. Secondly, more diverse sky conditions should be tested. Thirdly, the evaluation metrics are limited to MAE, RMSE and R in this study. Other metrics, such as Mean bias error (MBE), Normalized Root Mean Square Error (nRMSE), Mean Absolute Percentage Error (MAPE) could be applied.

Conclusion

This study developed a hybrid nowcasting method for Global Horizontal Irradiance (GHI) using an advanced CNN model with ResNet structure to identify the ground cloud images information collected by an open database – NREL dataset. Several ResNet structures are compared to achieve an optimal nowcasting model for GHI. The results show that the ResNet structure could efficiently capture the significant information of cloud images and the ResNet-152 has the optimal performance on solar irradiance nowcasting. The final result also indicates that a low prediction error and high relative coefficient values are obtained. The accomplishment of the nowcasting model apparently decreases the difficulty of solar irradiance forecast because it only needs to use cloud image. Nevertheless, considering the generalisation of this study, the proposed nowcasting model should be tested in various temporal horizon and weather conditions according to more evaluation metrics and optimised in future work.

Acknowledgement

This research has received support from the European Union's Horizon 2020 research and innovation programme under grant agreement No 768735 and Cardiff University's Global Challenges Research Fund HABITAT project. The authors thankfully acknowledge weather data and cloud images provided by National Renewable Energy Laboratory (NREL)'s Solar Radiation Research Laboratory (SRRL).

References

Alonso-Montesinos , J., Polo, J., Ballestrín, J., Batlles , F., & Portillo, C. (2019). Impact of DNI forecasting on CSP tower plant power production. *Renewable Energy, 138*, pp. 368-377.

Anderberg, M., & Sengupta, M. (2014). Comparison of Data Quality of NOAA's ISIS and SURFRAD Networks to NREL's SRRL-BMS. *Western Journal of Surgery Obstetrics & Gynecology, 58*(5), pp. 941-946.

Antonanzas, J., Osorio, N., Escobar, R., Urraca, R., Martinez-de-Pison, F., & Antonanzas-Torres, F. (2016). Review of photovoltaic power forecasting. *Solar Energy, 36*(15), pp. 78-111.

Bone, V., Pidgeon, J., Kearney, M., & Veeraragavan, A. (2018). Intra-hour direct normal irradiance forecasting through adaptive clear-sky modelling and cloud tracking. *Solar Energy, 159*, pp. 852-867.

Caldas, M., & Suarez , R. A. (2019). Very short-term solar irradiance forecast using all-sky imaging and real-time irradiance measurements. *Renewable Energy, 143*, pp. 1643-4658.

Chen, L., Hu, D., & Li, Y. (2019). Scoping Low-Cost Measures to Nowcast Sub-Hourly Solar Radiations for Buildings. *IOP Conference Series Earth and Environmental Science, 329*, 012041.

Diagne, M., David, M., Lauret, P., Boland, J., & Schmutz, N. (2013). Review of solar irradiance forecasting methods and a proposition for small-scale insular grids. *Renewable and Sustainable Energy Reviews, 27*, pp. 65-76.

Dong, B., & Lam, K. P. (2014). A real-time model predictive control for building heating and cooling systems based on the occupancy behavior pattern detection and local weather forecasting. *Building Simulation, 7*, pp. 89-106.

Du, H., Bandera, C. F., & Chen, L. (2019). Nowcasting Methods For Optimising Building Performance. *Building Simulation* (pp. 1-9). Rome,Italy: International building performance simulation association.

Gentile, S., Paola, F. D., Cimini, D., Gallucci, D., Geraldi, E., Larosa, S., . . . Romano, F. (2020). 3D-VAR Data Assimilation of SEVIRI Radiances for the Prediction of Solar Irradiance in Italy Using WRF Solar Mesoscale Model—Preliminary Results. *Remote Sensor, 12*, p. 920.

Guermoui, M., Melgani, F., & Danilo, C. (2018). Multi-step ahead forecasting of daily global and direct solar radiation: A review and case study of Ghardaia region. *Journal of Cleaner Production, 201*(10), pp. 716-734.

He, K., Zhang, X., Ren, S., & Sun, J. (2016). Deep Residual Learning for Image Recognition. *2016 IEEE Conference on Computer Vision and Pattern Recognition (CVPR. 1*, pp. 770-778. Las vagas,USA: IEEE computer society.

Kallio-Myers, V., Riihelä, A., Lahtinen, P., & Lindfors, A. (2020). Global horizontal irradiance forecast

for Finland based on geostationary weather satellite data. *Solar Energy, 198*, pp. 68-80.

Kim, W., Katipamula, S., & Lutes, R. (2020). Application of intelligent load control to manage building loads to support rapid growth of distributed renewable generation. *Sustainable Cities and Society*(53), p. 101898.

Kong, W., Jia, Y., Dong, Z., Meng, K., & Chai, S. (2020). Hybrid approaches based on deep whole-sky-image learning to photovoltaic generation forecasting. *Applied Energy, 280*, p. 115875.

Krizhevsky, A., Sutskever, I., & Hinton, G. (2012). Imagenet classification with deep convolutional neural networks. *Advances in Neural Information Processing Systems*(1), pp. 1097-1105.

Kummert, M., André, P., & Nicolas, J. (2001). Optimal heating control in a passive solar commercial building. *Solar Energy, 69*(6), pp. 103-116.

Kwak, Y., Seo, D., Jang, C., & Huh, J.-H. (2013). Feasibility study on a novel methodology for short-term real-time energy demand prediction using weather forecasting data. *Energy and Buildings, 57*, pp. 250-260.

Kwon, Y., Kwasinski, A., & Kwasinski, A. (2019). Solar Irradiance Forecast Using Naïve Bayes Classifier Based on Publicly Available Weather Forecasting Variables. *energies, 12*, pp. 1529-.

Leelaruji , T., & Teerakawanich, N. (2020). Short Term Prediction of Solar Irradiance Fluctuation Using Image Processing with ResNet. *2020 8th International Electrical Engineering Congress (iEECON)， IEEE*, (pp. 1-4).

Leirpoll, M. E., Næss, J. S., Cavalett, O., Dorber, M., Hu, X., & Cherubini, F. (2021). Optimal combination of bioenergy and solar photovoltaic for renewable energy production on abandoned cropland. *Renewable Energy, 468*, pp. 45-56.

Miller, S. D., Rogers, M. A., Haynesa, J. M., Sengupta, M., & Heidinger, A. K. (2018). Short-term solar irradiance forecasting via satellite/model coupling. *Solar Energy, 168*, pp. 102-117.

Miriyala, S. S., Nagalla, S. H., & Mitra, K. (2019). Comparative Study of Optimal Long Short Term Memory Networks for One Day Ahead Solar Irradiance Hourly Forecast. *2019 Sixth Indian Control Conference (ICC)*, (pp. 238-243). IIT Hyderabad, India.

Pereira, R., Santos, C. S., & Rocha, A. (2019). Solar irradiance modelling using an offline coupling procedure for the Weather Research and Forecasting (WRF) model. *Solar Energy, 188*, pp. 339-352.

Perez, R., Ineichen, P., Maxwell, E., Seals, R., & Zelenka, A. (1992). Dynamic global-to-direct irradiance conversion models. *ASHRAE Transactions, 98*, 354-369.

Ronan, C., & Jason, W. (2008). A Unified Architecture for Natural Language Processing: Deep Neural Networks with Multitask Learning. *Proceedings of the 25th International Conference on Machine Learning. ICML '08* (pp. 160–167). New York, USA: ACM.

Song, J., & Song, S. (2020). A framework for analysing city-wide impact of building-integrated renewable energy. *Applied Energy, 276*, p. 115489.

SORKUN, M. C., İNCEL, Ö. D., & PAOLI, C. (2020). Time series forecasting on multivariate solar radiation data using deep learning (LSTM). *Turkish Journal of Electrical Engineering & Computer Sciences, 28*, pp. 211-223.

Stein, J. S., Holmgren, W. F., Forbess, J., & Hansen, C. W. (2016). PVLIB: Open source photovoltaic performance modeling functions for Matlab and Python. *In: 2016 IEEE 43rd photovoltaic specialists conference*, pp. 3425-3430.

Stoffel, T., & Andreas, A. (1981). *NREL Solar Radiation Research Laboratory (SRRL): Baseline Measurement System (BMS); Golden, Colorado (Data)*. National Renewable Energy Lab. (NREL), Golden, CO (United States).

Wang, F., Xuan, Z., Zhen, Z., Li, Y., Li, K., Zhao, L., . . . Catalão, J. P. (2020). A minutely solar irradiance forecasting method based on real-time sky image-irradiance mapping model. *Energy Conversion and Management, 220*, p. 113075.

Wu, Z., Li, Q., & Xia, X. (2021). Multi-timescale Forecast of Solar Irradiance Based on Multi-task Learning and Echo State Network Approaches. *IEEE TRANSACTIONS ON INDUSTRIAL INFORMATICS, 17*(1), pp. 300-310.

Yang, D., Kleissl, J., Gueymard, C. A., Pedro, H. T., & Coimbra, C. F. (2018). History and trends in solar irradiance and PV power forecasting: A preliminary assessment and review using text mining. *Solar Energy, 60*(101), pp. 60-101.

Yu, Y., Cao, J., Wan, X., Zeng, F., Xin, J., & Ji, Q. (2018). Comparison of short-term solar irradiance forecasting methods when weather conditions are complicated. *Journal Renewable Sustainable Energy, 10*, pp. 053501 1-11.

Zalata , M. A., Robandi, I., & Riawan, D. C. (2018). New Model for Hourly Solar Radiation Forecasting using ANN for Java Island, Indonesia. *International Conference on Computer Engineering, Network and Intelligent Multimedia*, (pp. 294-298). surabaya, Indonesia.